Flexible, stretchable and conductive PVA/PEDOT:PSS composite hydrogels prepared by SIPN strategy

Yun-Fei Zhang [a,b], Ming-Ming Guo [a,c], Ya Zhang [a], Chak Yin Tang [b,*], Can Jiang [a], Yuqing Dong [b], Wing-Cheung Law [b], Fei-Peng Du [a,**]

[a] School of Materials Science and Engineering, Wuhan Institute of Technology, Wuhan, 430205, China
[b] Department of Industrial and Systems Engineering, The Hong Kong Polytechnic University, Hong Kong, China
[c] School of Chemical Sciences, University of Chinese Academy of Sciences, Beijing, 100049, China

ARTICLE INFO

ABSTRACT

Stretchable conductive hydrogels have received significant attention due to their possibility of being utilized in wearable electronics and healthcare devices. In this work, a semi-interpenetrating polymer network (SIPN) strategy was employed to fabricate a set of flexible, stretchable and conductive composite hydrogels composed of polyvinyl alcohol (PVA) in the presence of glutaraldehyde as the crosslinker, HCl as the catalyst and poly(3,4-ethylenedioxythiophene):polystyrenesulfonate (PEDOT:PSS) as the conductive medium. The results from FTIR, Raman, SEM and TGA indicate that a chemical crosslinking network and interactions of PVA and PEDOT:PSS exist in the SIPN hydrogels. The swelling ratio of hydrogels decreased with increasing content of PEDOT:PSS. Due to the chemical crosslinking network and interactions of PVA and PEDOT:PSS, PVA networks semi-interpenetrated with PEDOT:PSS exhibited excellent tensile and compression properties. The tensile strength and elongation at breakage of the composite hydrogels with 0.14 wt% PEDOT:PSS were 70 KPa and 239%, respectively. The compression stress of the composite hydrogels with 0.14 wt% PEDOT:PSS at a strain of 50% was about 216 KPa. The electrical conductivity of the hydrogels increased with increasing PEDOT:PSS content. The flexible, stretchable and conductive properties endow the composite hydrogel sensor with a superior gauge factor of up to 4.4 (strain: 100%). Coupling the strain sensing capability to the flexibility, good mechanical properties and high electrical conductivity, we consider that the designed PVA/PEDOT:PSS composite hydrogels have promising applications in wearable devices, such as flexible electronic skin and sensitive strain sensors.

1. Introduction

Flexible polymer materials have been widely used in wearable electronic devices, such as electronic skin, electrical sensors, electronic encapsulation and healthcare equipment, and have received much attention and achieved a fast development [1–4]. Electro-conductive polymer hydrogels (ECHs) are typical, flexible and electro-conductive materials with a three-dimensional network, and are considered as suitable candidates for the fabrication of wearable electronic devices [5–7]. For the fabrication of ECHs, electro-conductive fillers, such as poly(3,4-ethylenedioxythiophene):poly(styrenesulfonate) (PEDOT:PSS) [8], polyaniline [9,10], polypyrrole [11,12] and carbon materials [13–15] are commonly imbedded in the polymer hydrogel network to endow electro-conductivity properties. As one of the most promising electro-conductive polymers, PEDOT:PSS has high electrical conductivity, chemical stability, processability in aqueous solutions and environmental friendliness, and has been widely used in conductive hydrogels for sensors [16,17]. However, most ECHs currently suffer from weak mechanical strength, biological incompatibility and relatively complicated preparation methods, which cannot meet the demands in practical applications in wearable electronics [18–20].

Poly (vinyl alcohol) (PVA) hydrogels have the advantages of low cost, good mechanical properties, high water content and good biocompatibility [21–24], and have been widely used as wearable sensors [25], soft actuators [26], wound dressings [27] and drug delivery carriers [28]. Regarding the characteristics of high flexibility and stretchability, the PVA hydrogel has been deemed a good candidate for soft strain sensors matrixes [29]. Currently, how to obtain flexible,

* Corresponding author.
** Corresponding author.
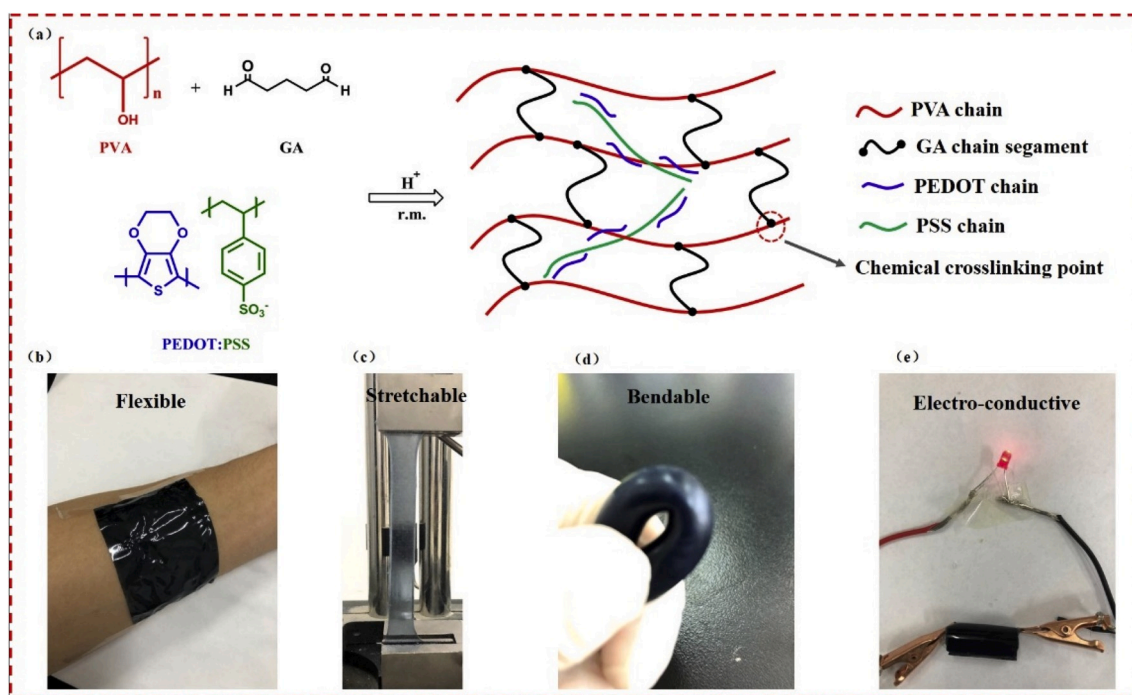*E-mail addresses:* cy.tang@polyu.edu.hk (C.Y. Tang), hsdfp@163.com (F.-P. Du).

Fig. 1. (a) Synthesis mechanism of the SIPN PVA/PEDOT:PSS hydrogel; Demonstration of the (b) flexibility, (c) stretchability, (d) bendability and (e) electro-conductivity of hydrogels.

stretchable, conductive and strain-sensitive PVA ECHs has been a key issue in the field of soft strain sensors. Liao et al. and Liu et al. reported an artificial epidermal skin sensor based on a composite of PVA/carbon nanotubes/polydopamine and a composite of PVA/polydopamine, respectively [2,30]. Jing et al. reported a transparent, stretchable, and self-healing PVA/cellulose nanofibril ECHs for pressure and strain sensors by dual-crosslinked networks [31]. However, in the practical application of soft strain sensors, most reported PVA ECHs are often plagued with problems such as weak mechanical strength [25], low electro-conductivity [32], or complicated preparation methods [32]. Therefore, it is desirable to develop a facile method to prepare PVA ECHs with comprehensive performance for use as soft strain sensors.

A semi-interpenetrating polymer network (SIPN) strategy has been proven to be a facile technique to fabricate stable conductive hydrogels with excellent mechanical properties [33,34]. In this study, we demonstrate that flexible, stretchable and conductive PVA/PEDOT:PSS composite hydrogels can be successfully fabricated by penetrating the conductive agent PEDOT:PSS polymer chain into the PVA network and forming SIPN structures through a simple two-step method of mixing and in-situ crosslinking. The incorporation of small amounts of PEDOT:PSS considerably improve the mechanical properties and electro-conductivity for the PVA/PEDOT:PSS composite hydrogels. The flexible, stretchable and conductive properties produce a composite hydrogel sensor with a superior gauge factor of up to 4.4 (strain: 100%). The designed PVA/PEDOT:PSS composite hydrogels show promise for applications in wearable devices, such as flexible electronic skin and sensitive strain sensors.

2. Experimental

2.1. Materials

PEDOT:PSS (Clevios PH1000, PEDOT:PSS mass ratio of 1:2.5 by weight with 1.0–1.3% solid content in water) was purchased from Sigma-Aladdin Industrial Corporation (Shanghai, China). Poly (vinyl alcohol) (PVA, polymerization degree: 1700, alcoholysis degree: 98.0–99.0%), dimethyl sulfoxide (DMSO), glutaraldehyde solution (GA,

25.0 wt%) and hydrochloric acid (37.5 wt%) were purchased from Sinopharm Chemical Reagent Co, Ltd (Shanghai, China). All the chemicals were of analytical purity and directly used without further purification.

2.2. Preparation of PVA/PEDOT:PSS hydrogels

A PVA solution with a concentration of 8.0 wt% was obtained by dissolving 0.8 g of PVA in 9.2 mL of deionized water under mechanical stirring at 95 °C. Then 2.0 mL DMSO, a certain amount of PEDOT:PSS and 0.1 mL 12.5 wt% GA solution were added into the prepared cooled PVA solution via a high speed disperser for a further 10 min, and under ultrasonic treatment for a further 10 min, respectively. Secondly, 0.1 mL 10.0 wt% hydrochloric acid was slowly added into the above mixed solution under ultrasonic treatment for 10 min. Finally, the PVA/PEDOT:PSS hydrogel was obtained by casting the solution in a self-made mold and crosslinking the PVA solution at room temperature for 6 h. Here, the concentrations of PEDOT:PSS were selected as 0.00 wt%, 0.04 wt%, 0.07 wt%, 0.10 wt% and 0.14 wt%, identified as PVA-PP-0, PVA-PP-4, PVA-PP-7, PVA-PP-10, PVA-PP-14.

2.3. Characterizations

Composition and microstructures test. Fourier transform infrared (FT-IR) spectra were obtained using a FT-IR spectrometer (Nicolet 6700, Thermo scientific, USA) with an attenuated total reflectance (ATR) attachment. Raman spectra were recorded for all the samples at ambient conditions on a Raman spectrometer (DXR, Thermo scientific, USA), with excitation by laser beam of 532 nm wavelength. Thermogravimetric analysis (TGA) was carried out on a TGA 5500 system (TA Instruments CO., USA). The heating rate was 10 °C/min from 30 °C to 700 °C under nitrogen flow. The morphology and microstructures were characterized by scanning electron microscopy (SEM) (Phillips XL30, FEI Company, USA). The hydrogel samples for the FTIR, Raman, TG and SEM tests were frozen for 24 h, then vacuum freeze-dried at −55 °C (Free Zone 4.5® Liter Freeze Dry System 77500 Series) for 24 h.

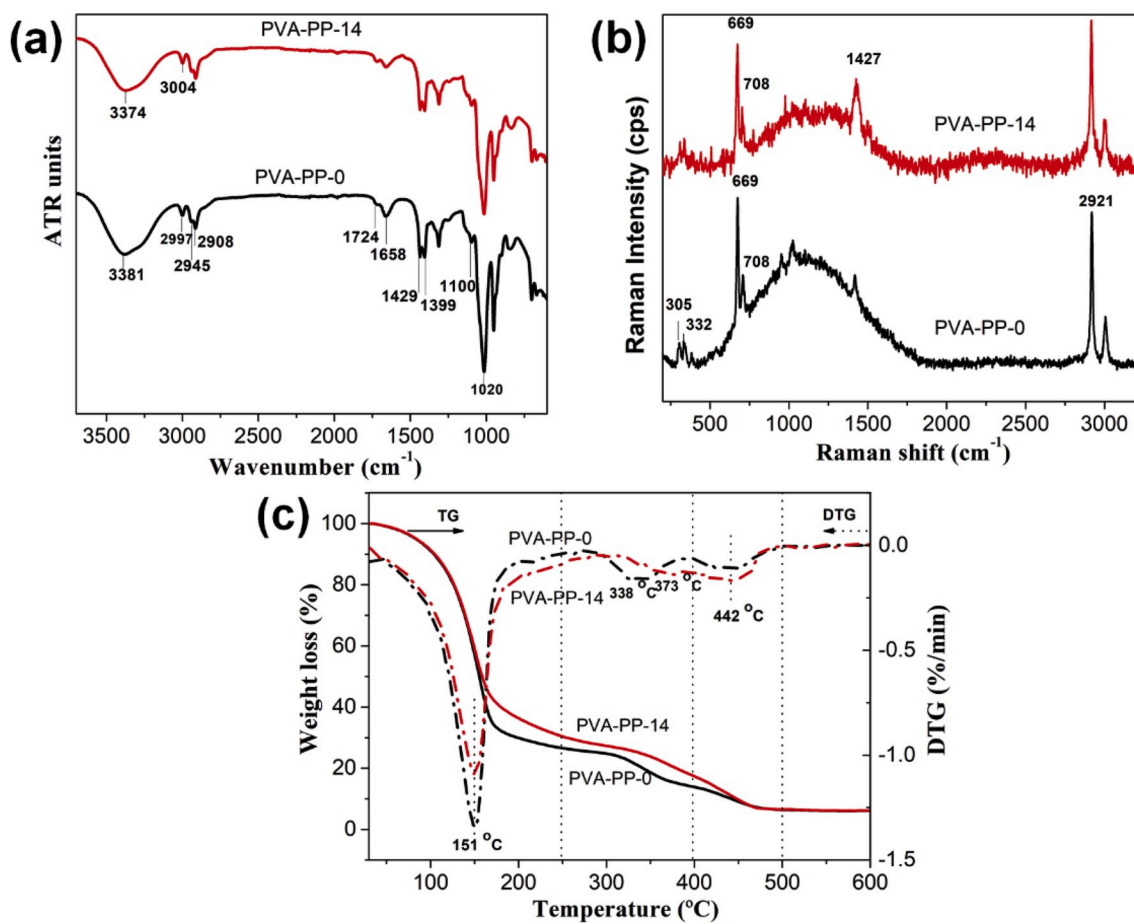**Swelling behavior.** The swelling behavior of the freeze-dried

Fig. 2. FT-IR spectra (a), Raman spectra (b) and TG curves (c) of the composite hydrogels.

hydrogels was analyzed by recording their weight change in water over time at room temperature. The swelling ratio (SR) was calculated by the equation $SR = (m_t - m_0)/m_0$, where m_0 is the initial weight of the dried hydrogels and m_t is the weight of the hydrogel at different time intervals.

Mechanical test. Tensile testing of the composite hydrogels was conducted with reference to ASTM D638 standard, with slight modification [35,36]. Uniaxial tensile tests of rectangular hydrogel strips (50 mm × 15 mm × 1.5 mm) were performed on an Instron 5567 universal testing machine at a crosshead speed of 30 mm/min. The compression tests were conducted on as-prepared cylinder hydrogel samples (length = 14 mm and diameter = 25 mm) at 7 mm/min and the compression strain limit was set as 50%. Both the tensile and compression tests were operated under a 250 N load cell (Instron Inc, USA) at room temperature.

Strain sensing ability tests. The electrical testing of the composite hydrogels was conducted follow up Ref [37], with slight modifications [37]. Two individual copper adhesive tapes acting as electrodes were attached on the two sides of the composite hydrogel strips (50 mm × 15 mm × 1.5 mm), respectively. The distance between the two electrodes was about 40 mm. The resistance changes of the composite hydrogels in different tensile states were obtained by using a Keithley 2000 (Keithley, USA) instrument. The relative change of the resistance was calculated on the basis of the current: $\Delta R/R_0 = (R_s - R_0)/R_0$, where R_0 and R_s are the initial resistance of the strain sensor and the resistance under tensile deformation, respectively.

3. Results and discussion

3.1. Preparation and characterization of PVA/PEDOT:PSS

A semi-interpenetrating polymer network (SIPN) strategy was employed to fabricate a type of hydrogel composed of polyvinyl alcohol (PVA) in the presence of GA as the crosslinker, HCl as the catalyst and poly(3,4-ethylenedioxythiophene):polystyrenesulfonate (PEDOT:PSS) as the conductive medium, as schematically illustrated in Fig. 1a. The SIPN structure of the composite hydrogel is shown in Fig. 1a, and was constructed by cross-linking the PVA and linear PEDOT and PSS. PEDOT:PSS is a mixture of highly conductive polymers, where PSS possesses a negative charge due to the deprotonation of the sulfonyl groups while PEDOT carries a positive charge. Glutaraldehyde serves as the cross-linker to facilitate the formation of a robust PEDOT:PSS network in the PVA, providing the conductivity and flexibility to the polymer matrix [38]. Fig. 1b, c, and d show that the fabricated PVA/-PEDOT:PSS hydrogels demonstrate good flexibility, stretchability, and bendability, respectively. The fabricated PVA/PEDOT:PSS hydrogel specimen exhibited good electrical conductivity, as shown in Fig. 1e. In order to improve the electro-conductivity of the composite hydrogels, 2.0 mL of polar solvent DMSO was used as a secondary dopant for partial phase separation of the excess insulating PSS, according to Refs. [39,40].

IR spectroscopy was used to confirm the functional groups in the composite hydrogels and to investigate the formation of the crosslinking network from the blends with GA. The IR spectra of PVA-PP-0 hydrogel and PVA-PP-14 hydrogel are shown in Fig. 2a. For pure PVA (PVA-PP-0), the broad and strong peak at 3381 cm^{-1} is assigned to the symmetrical stretching vibration of the -OH groups. The peak at 2997 cm^{-1} is due to the stretching vibration of the C-Hs of the PVA. The shoulder peaks at
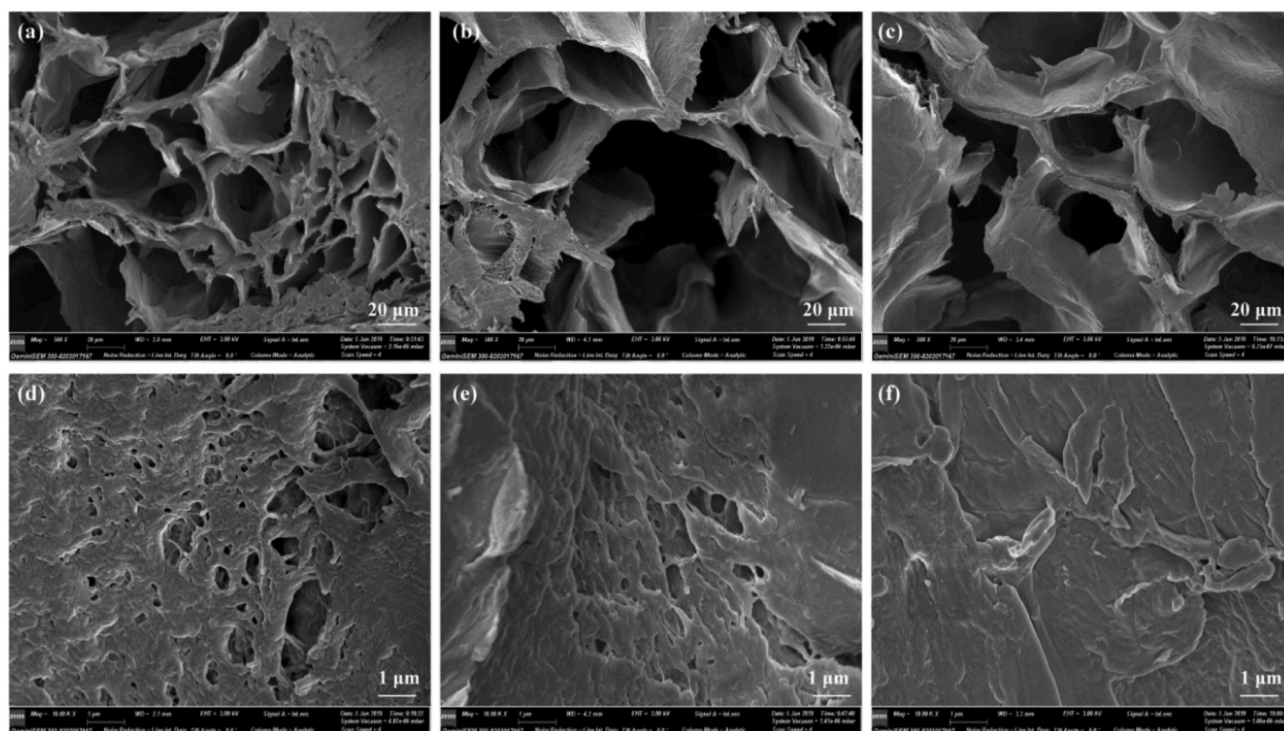
Fig. 3. FE-SEM images of the hydrogel: (a, d) PVA-PP-0, (b, e) PVA-PP-7, (c, f) PVA-PP-14.

$2945 \, \text{cm}^{-1}$ and $2908 \, \text{cm}^{-1}$ were assigned to the C-Hs of aldehyde groups and C-Hs of alkyl groups, which indicate the incorporation of aldehyde molecules into the PVA network [41]. The peak at $1724 \, \text{cm}^{-1}$ corresponded to the acetyl residue of the PVA molecules [42]. The broad peak range from 900 cm to 1 to 1500 cm-1 has been reanalyzed in the manuscript. Peaks at 1100 cm-1 and 1020 cm-1, represent the -C-O-C-O-C- acetal structure, indicating the acetal reaction of PVA and GA under acidic conditions. The shoulder peaks at 1429 cm-1 and 1399 cm-1 are assigned to the bending vibration of C-Hs of aldehyde groups of PVA [41]. As for PVA-PP-14, the IR absorption peak is similar to that of PVA-PP-0 due to the main skeleton of PVA hydrogel matrix. In addition, the peaks at about $1520 \, \text{cm}^{-1}$ and $1200 \, \text{cm}^{-1}$ are attributed to the stretching vibration of C=C in the thiophene ring and ethylenedioxy group on the PEDOT, respectively [43]. The peak at $3004 \, \text{cm}^{-1}$ is assigned to the stretching vibration of =C-H of PSS. Particularly, the -OH stretching peak shifts to a lower wavenumber, indicating that the hydrogen bonding interactions between the hydroxyl groups on the PVA molecular chains were reduced by the interactions between PVA and PEDOT:PSS.

The Raman spectra of the PVA-PP-0 hydrogel and PVA-PP-14 are shown in Fig. 2b. The peak at $2921 \, \text{cm}^{-1}$ corresponds to the stretching vibration of the C-C of the PVA. The peaks at $310 \, \text{cm}^{-1}$ and $335 \, \text{cm}^{-1}$ are assigned to the deformation vibration of the GA carbon chain, indicating the existence of GA segments in the hydrogels. The peak at $1427 \, \text{cm}^{-1}$ was assigned to the stretching vibration of $C_\alpha = C_\beta$ on the five-member thiophene ring of PEDOT [44]. The scattering peak of C-C and C-O stretching and bending vibrations of PVA overlapped and formed a broad peak range from $900 \, \text{cm}^{-1}$ to $1500 \, \text{cm}^{-1}$. The intensity of the broad peak decreased after the incorporation of PEDOT:PSS, which might be due to the weak hydrogen bonding interactions between the hydroxyl groups on the PVA molecular chains decreasing due to the interactions between the PVA and PEDOT:PSS.

The thermal degradation properties of PVA-PP-0 and PVA-PP-14 were measured to evaluate the thermal stability of the composite hydrogels and to investigate the intermolecular interaction between the PVA and PEDOT:PSS. The TG and DTG results from Fig. 2c both exhibit
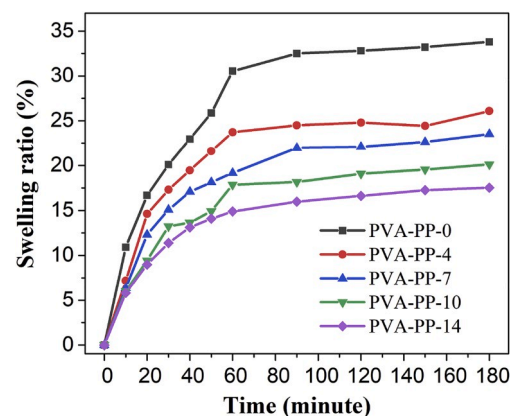

Fig. 4. Effect of PEDOT:PSS concentration on the swelling ratio of composite hydrogel.

the degradation of PVA-PP-0 and PVA-PP-14 which shows three stages of degradation. The first weight loss in the temperature region 100–250 °C is due to the loss of free water molecules and water molecules from the etherification reaction of the polyvinyl alcohol -OH groups [45]. The second weight loss in the temperature region 250–400 °C is due to the decomposition of polyvinyl alcohol main-chain and the third weight loss around 442 °C is due to the decomposition of the residual main-chain decomposition [46]. The maximum rate of the weight loss temperature for the decomposition of polyvinyl alcohol increases from 338 °C to 373 °C after incorporation of PEDOT:PSS, indicating that the disintegration of PVA is impeded when PEDOT:PSS is coated on the surfaces of the PVA.

Fig. 3 shows the FE-SEM images of the freeze-dried PVA/PEDOT:PSS hydrogels with different PEDOT:PSS concentrations. The prepared hydrogels have the typical micro-porous structure at low magnification, as shown in Fig. 3(a, b and c), which arises from the freeze-drying formation process of the dried hydrogels [47]. Fig. 3(d, e and f) shows that
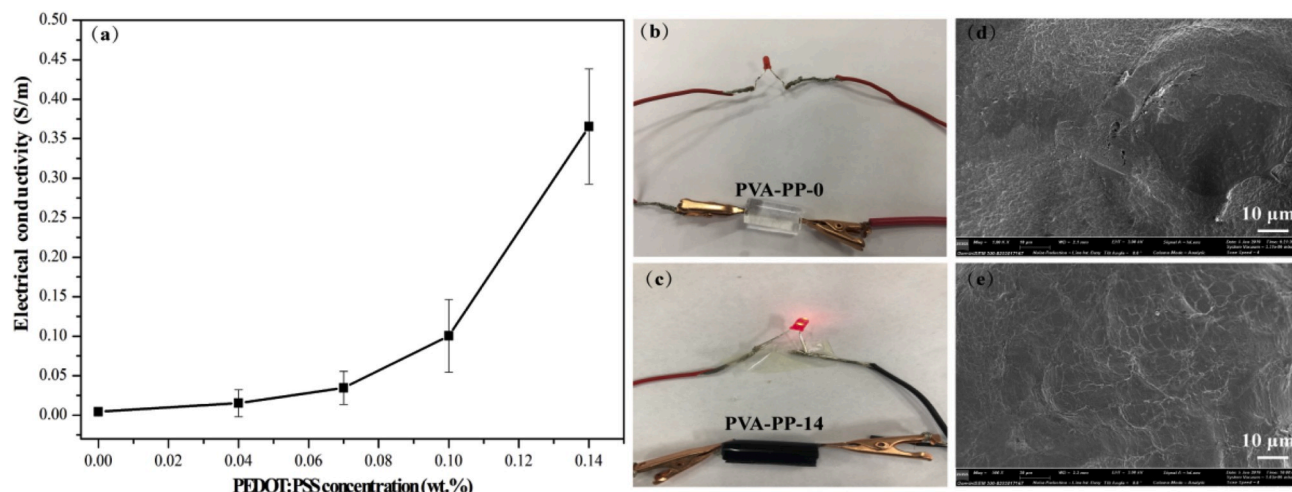
Fig. 5. (a) The electrical conductivity of hydrogel at different concentrations of PEDOT:PSS. Photographs of PVA-PP-0 (b) and PVA-PP-14 (c) connected in series with a red LED indicator in the circuit. FE-SEM images of PVA-PP-0 (d) and PVA-PP-7 (e).

the surfaces of PVA/PEDOT:PSS hydrogel are relatively smooth and dense in structure. Moreover, Fig. 3(d, e and f) also shows that the size and number of micro-pores in the PVA/PEDOT:PSS hydrogel are decreasing with increasing amounts of PEDOT:PSS, indicating that the PEDOT and PSS chains have been successfully penetrated into the PVA crosslinking network to form an semi-interpenetrating network structure.

In order to study the effect of PEDOT:PSS on the hydrophilicity of the composite hydrogels, the swelling ratios of the composite hydrogels with different PEDOT:PSS concentrations were studied. Fig. 4 shows that the swelling ratio of the composite hydrogels clearly decreased with the increasing PEDOT:PSS concentration. The hydrogels almost reached the swelling equilibrium after 90 min, and the maximum swelling ratios of PVA-PP-0, PVA-PP-4, PVA-PP-10 and PVA-PP-14 were about 34%, 25%, 22%, 19% and 17%, respectively. The maximum swelling ratio of the PVA-PP-0 hydrogel is about twice as large as that of the PVA-PP-14. On the one hand, PEDOT:PSS is more hydrophobic than the hydrogel matrix PVA [48]. On the other hand, the PEDOT and PSS chains inside the composite hydrogels, acting as physical reinforcements, contribute to a decrease in the degree of swelling. This also agrees with the results shown in Fig. 3 that the hydrogel containing more PEODT:PSS has fewer and smaller micro-pores, which impedes more water molecules travelling through the hydrogel freely, and remain inside the micro-pores.

3.2. Electrical conductivity

Fig. 5a shows the changes in the electrical conductivity of the composite hydrogel with various PEDOT:PSS concentrations. It can be seen in Fig. 5a that the electrical conductivity of composite hydrogel increases with increasing concentrations of the PEDOT:PSS conductive dopant, from $4.5 \times 10^{-3}\,\text{S}\,\text{m}^{-1}$ (PVA-PP-0) to $0.36\,\text{S}\,\text{m}^{-1}$ (PVA-PP-14) when the PEDOT:PSS concentration increases from 0.0 wt% to 1.4 wt%. When the concentration of the conductive medium PEODT:PSS is higher than 1.0 wt%, the electrical conductivity increases sharply, as shown in Fig. 5a, indicating the formation of the percolation network [49,50]. A driving voltage below 2 V cannot light up the LED in specimen PVA-PP-0 specimen, as shown in Fig. 5b. It can be readily observed from Fig. 5c that the LED was lit when the PVA-PP-0 specimen is replaced with the PVA-PP-14 specimen. Fig. 5d and e indicate that the prepared PVA-PP-0 and PVA-PP-14 have dense and smooth structures, and Fig. 5e shows that the PEDOT:PSS is uniformly dispersed in the PVA hydrogel matrix, contributing to the enhancement of the electrical conductivity.

3.3. Mechanical properties

Tensile tests were performed to examine the effect of the PEDOT:PSS concentration on the tensile properties of the composite hydrogel, and the results are shown in Fig. 6a. The tensile strength and the elongation at breakage of the PVA-PP-0 hydrogel are about 30 KPa and 114%, respectively. When the content of PEDOT:PSS increased from 0.00 wt%
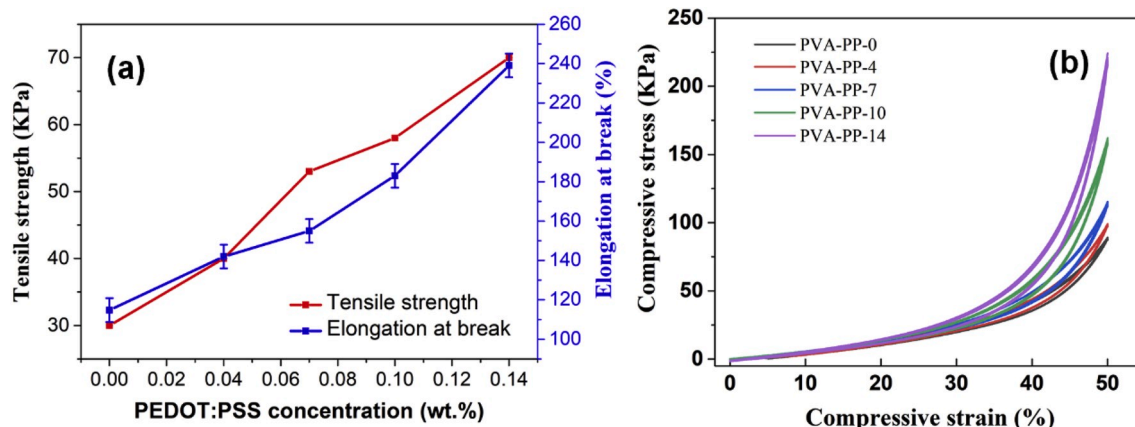

Fig. 6. The tensile properties (a) and compression stress-strain curve (b) of the composite hydrogels.
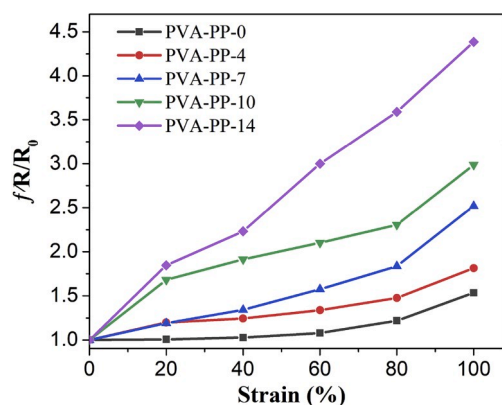
Fig. 7. Relative resistance changes of the PVA/PEDOT:PSS composite hydrogel sensors as a function of applied strain.

to 0.14 wt%, the tensile strength and elongation at breakage of the PVA/PEDOT:PSS hydrogels increased from 30 to 70 kPa and 114%–239%, respectively. The recoverable properties of the hydrogels at the same strain level (50%) were investigated by the loading-unloading tests shown in Fig. 6b. It can be seen in Fig. 6b that there is almost no hysteresis for the composite hydrogels and the sample fully recovers to its original state after unloading, exhibiting typical rubber elastic behavior. Fig. 6b also shows that the compressive stress of the composite hydrogels at the same strain level is increased with increasing concentrations of PEDOT:PSS. The compression stresses of the PVA-PP-0 and PVA-PP-14 specimens at a strain of 50% are 87.5 KPa and 215.7 KPa, respectively.

The good mechanical properties of the composite hydrogels may be due to the good dispersion of the PEDOT:PSS in the PVA hydrogels and the SIPN structure formed in the composite hydrogels. Under deformation, the covalent crosslinking maintains the original network configuration, and segment movements of the PVA chain, glutaraldehyde chain and PEDOT:PSS chains are combined to dissipate energy and transfer stress from the PVA matrix to the PEDOT:PSS reinforcement [51]. Furthermore, hydrogen bonding between the PVA matrix and reinforcement PEDOT:PSS are also thought to be one of the factors that improve the mechanical properties of the composite hydrogels [52]. The hybrid chemical crosslinking and hydrogen bonding interactions in SIPN networks endow PVA/PEDOT:PSS composite hydrogels with excellent mechanical properties.

3.4. Strain-sensitive behaviors

To evaluate the practicability of the PVA/PEDOT:PSS hydrogel for

use in wearable sensing applications, the strain-$\Delta R/R_0$ of the composite hydrogel was studied and the results are shown in Fig. 7(a). It can be noted that all the $\Delta R/R_0$ curves of the composite hydrogels increased with increasing applied strain (0–100%), suggesting that the electrical conductivity of the composite hydrogel was sensitive to the applied strain. When the strain was increased, the space between the conductive medium in the hydrogel was enlarged, causing increased resistance of the hydrogel. Furthermore, the $\Delta R/R_0$ of the composite hydrogel at the same strain level increased with the increasing concentrations of PEDOT:PSS, indicating that the higher the electrical conductivity of the composite hydrogel, the more the strain sensitivity of the composite hydrogel. For example, when the strain was 100%, the $\Delta R/R_0$ values of the PVA-PP-0, PVA-PP-7 and PVA-PP-14 were 1.53, 2.52 and 4.38, respectively. The gauge factor (GF) is used to quantitatively evaluate the sensitivity of a strain sensor, and is estimated by following formula: GF= $(R_s$-$R_0)/(R_0\varepsilon)$, where R_s, R_0 and ε represent the testing resistance, the initial resistance, and the strain, respectively. Fig. 7 illustrates that the GF of the composite hydrogel is improved with increasing PEDOT:PSS content, reaching 4.38 (strain: 100%) in the experiment. Table 1 shows a comparison of the fabrication method and GF value obtained from this work as compared with the results of some typical types of strain sensors. Amongst the various investigated conductive materials used in the composite hydrogel, as shown in Table 1, PEDOT:PSS is seen to be the most useful polymeric material for wearable healthcare sensors because of its excellent chemical stability, optical transparency, electrical properties, processability in aqueous solutions, environmental friendliness and biocompatibility [53]. It was reported that PVA/PEDOT:PSS in the form of nanofibers exhibits a high GF [57] due to an series effect on resistance. In our work, the SIPN PVA/PEDOT:PSS composite hydrogels were fabricated in strip form by the solution-cast method. This method is environmental friendly, cost effective, and suitable for large scale of production. Moreover, it is found that the GF values with the small PEDOT:PSS doping levels prepared in this work are superior to most of the reported gel-based strain sensors with similar configurations, and exhibit high potential for producing sensitive and flexible strain sensors.

4. Conclusions

In summary, flexible, stretchable and conductive PVA/PEDOT:PSS composite hydrogels have been successfully fabricated by the SIPN strategy. The PVA/PEDOT:PSS composite hydrogel and the preparation method demonstrated in this study are environmentally friendly, cost effective, and suitable for large scale production. The SIPN structures play a significant role in the properties of the PVA/PEDOT:PSS, such as the swelling ratio, mechanical properties and relative resistance changes. The prepared PVA/PEDOT:PSS composite hydrogels exhibited

Table 1
A summary of some high-performance flexible strain sensors.

Hydrogel matrix	Conductive medium	Gauge factor (tensile strain)	Comment	Ref
PVA/poly dopamine	Reduced graphene oxide	1.0 (100%)	Dynamic H bonding crosslinking; Solution casting method	[32]
Polyacrylic acid (PAA)	Al^{3+}	4.9 (65%–75%)	Chemical crosslinking; Dynamic coordination	[54]
PAA	Polyaniline	11.6 (100%)	Physical crosslinking; Solution casting method	[55]
PAA	PEDOT:sulfonated lignin	7.0 (100%)	Chemical crosslinking; Solvent replacement strategy	[56]
Polyvinyl alcohol (PVA)	Single wall carbon nanotubes; Silver nanowire	1.51 (1000%) 2.25 (1000%)	Dynamic H bonding crosslinking; Solution casting method	[57]
PVA	PEDOT:PSS	396 (120%)	Electrospun technique	[58]
PVA/Polyvinylpyrrolidone	Fe^{3+}	0.478 (200%)	Dynamic Fe^{3+} crosslinking; Soft and hard hybrid networks	[59]
PVA	Multiwall carbon nanotubes	3.0 (100%)	Dynamic H bonding interaction; Infiltration technique	[60]
PVA	PEDOT:PSS	4.4 (100%)	Chemical crosslinking SIPN strategy	This work

excellent flexibility, stretchability, conductivity and relative high GF, demonstrating great potential for the preparation of lightweight and cheap wearable electronics, such as flexible electronic skin and sensitive strain sensors.

Declaration of competing interest

The authors declare that the work has not been published and/or accepted elsewhere, in whole or in part, and is not being submitted to any other journals for publication. All the authors listed have seen the manuscript and approved to submit to "***Polymer Testing***".

Acknowledgements

Appendix A. Supplementary data

Supplementary data to this article can be found online at https://doi.org/10.1016/j.polymertesting.2019.106213.

References

[1] P. Li, K. Sun, J. Ouyang, Stretchable and conductive polymer films prepared by solution blending, Acs Appl. Mater. Inter. 7 (2015) 18415–18423.

[2] M. Liao, P. Wan, J. Wen, M. Gong, X. Wu, Y. Wang, R. Shi, L. Zhang, Wearable, healable, and adhesive epidermal sensors assembled from mussel-inspired conductive hybrid hydrogel framework, Adv. Funct. Mater. 27 (48) (2017).

[3] A. Reghunadhan, J. Datta, M. Jaroszewski, N. Kalarikkal, S. Thomas, Polyurethane glycolysate from industrial waste recycling to develop low dielectric constant, thermally stable materials suitable for the electronics, Arab. J. Chem. (2018), https://doi.org/10.1016/j.arabjc.2018.03.012.

[4] X. Zhao, W.J. Han, C.S. Zhao, S. Wang, F.G. Kong, X.X. Ji, Z.Y. Li, X.A. Shen, Fabrication of transparent paper-based flexible thermoelectric generator for wearable energy Harvester using modified distributor printing technology, Acs Appl. Mater. Inter. 11 (2019) 10301–10309.

[5] R. Tong, G. Chen, D. Pan, H. Qi, R.a. Li, J. Tian, F. Lu, M. He, Highly stretchable and compressible cellulose ionic hydrogels for flexible strain sensors, Biomacromolecules 20 (5) (2019) 2096–2104.

[6] H. Gu, H. Zhang, C. Ma, H. Sun, C. Liu, K. Dai, J. Zhang, R. Wei, T. Ding, Z. Guo, Smart strain sensing organic-inorganic hybrid hydrogels with nano barium ferrite as the cross-linker, J. Mater. Chem. C 7 (8) (2019) 2353–2360.

[7] Y. Zhou, C. Wan, Y. Yang, H. Yang, S. Wang, Z. Dai, K. Ji, H. Jiang, X. Chen, Y. Long, Highly stretchable, elastic, and ionic conductive hydrogel for artificial soft electronics, Adv. Funct. Mater. 29 (1) (2019) 201806220.

[8] S. Cao, X. Tong, K. Dai, Q. Xu, A super-stretchable and tough functionalized boron nitride/PEDOT:PSS/poly(N-isopropylacrylamide) hydrogel with self-healing, adhesion, conductive and photothermal activity, J. Mater. Chem A 7 (14) (2019) 8204–8209.

[9] C.X. Hu, Y.L. Zhang, X.D. Wang, L. Xing, L.Y. Shi, R. Ran, Stable, strain-sensitive conductive hydrogel with antifreezing capability, remoldability, and reusability, Acs Appl. Mater. Inter. 10 (50) (2018) 44000–44010.

[10] H.B. Huang, J.L. Yao, L. Li, F. Zhu, Z.T. Liu, X.P. Zeng, X.H. Yu, Z.L. Huang, Reinforced polyaniline/polyvinyl alcohol conducting hydrogel from a freezing-thawing method as self-supported electrode for supercapacitors, J. Mater. Sci. 51 (2016) 8728–8736.

[11] H. Huang, J. Wu, X. Lin, L. Li, S. Shang, C.W.M. Yuen, G. Yan, Self-assembly of polypyrrole/chitosan composite hydrogels, Carbohydr. Polym. 95 (1) (2013) 72–76.

[12] Y. Bu, H.X. Xu, X. Li, W.J. Xu, Y.X. Yin, H.L. Dai, X.B. Wang, Z.J. Huang, P.H. Xu, A conductive sodium alginate and carboxymethyl chitosan hydrogel doped with polypyrrole for peripheral nerve regeneration, RSC Adv. 8 (20) (2018) 10806–10817.

[13] P.P. Li, Z.Y. Jin, L.L. Peng, F. Zhao, D. Xiao, Y. Jin, G.H. Yu, Stretchable all-gel-state fiber-shaped supercapacitors enabled by macromolecularly interconnected 3D graphene/nanostructured conductive polymer hydrogels, Adv. Mater. 30 (18) (2018) 201800124.

[14] E.P. Gilshteyn, S.T. Lin, V.A. Kondrashov, D.S. Kopylova, A.P. Tsapenko, A. S. Anisimov, A.J. Hart, X.H. Zhao, A.G. Nasibulin, A one-step method of hydrogel modification by single-walled carbon nanotubes for highly stretchable and transparent electronics, Acs Appl. Mater. Inter. 10 (33) (2018) 28069–28075.

[15] F.P. Du, E.Z. Ye, W. Yang, T.H. Shen, C.Y. Tang, X.L. Xie, X.P. Zhou, W.C. Law, Electroactive shape memory polymer based on optimized multi-walled carbon nanotubes/polyvinyl alcohol nanocomposites, Compos. B Eng. 68 (2015) 170–175.

[16] D. Kim, S.K. Ahn, J. Yoon, Highly stretchable strain sensors comprising double network hydrogels fabricated by microfluidic devices, Adv. Mater. Technol. 4 (7) (2019) 201800739.

[17] L. Wang, J. Zhang, Y. Guo, X. Chen, X. Jin, Q. Yang, K. Zhang, S. Wang, Y. Qiu, Fabrication of core-shell structured poly(3,4-ethylenedioxythiophene)/carbon nanotube hybrids with enhanced thermoelectric power factors, Carbon 148 (2019) 290–296.

[18] L. Han, X. Lu, M. Wang, D. Gan, W. Deng, K. Wang, L. Fang, K. Liu, C.W. Chan, Y. Tang, L.T. Weng, H. Yuan, A mussel-inspired conductive, self-adhesive, and self-healable tough hydrogel as cell stimulators and implantable bioelectronics, Small 13 (2017) 201601916.

[19] J. Hur, K. Im, S.W. Kim, J. Kim, D.Y. Chung, T.H. Kim, K.H. Jo, J.H. Hahn, Z.A. Bao, S. Hwang, N. Park, Polypyrrole/agarose-based electronically conductive and reversibly restorable hydrogel, ACS Nano 8 (2014) 10066–10076.

[20] C. Dispenza, C.L. Presti, C. Belfiore, G. Spadaro, S. Piazza, Electrically conductive hydrogel composites made of polyaniline nanoparticles and poly(N-vinyl-2-pyrrolidone), Polymer 47 (4) (2006) 961–971.

[21] F. Martinez-Gomez, J. Guerrrero, B. Matsuhiro, J. Pavez, In vitro release of metformin hydrochloride from sodium alginate/polyvinyl alcohol hydrogels, Carbohydr. Polym. 155 (2017) 182–191.

[22] H.J. Zhang, H.S. Xia, Y. Zhao, Poly(vinyl alcohol) hydrogel can autonomously self-heal, ACS Macro Lett. 1 (2012) 1233–1236.

[23] M. Guo, Y. Zhang, F. Du, Y. Wu, Q. Zhang, C. Jiang, Silver nanoparticles/polydopamine coated polyvinyl alcohol sponge as an effective and recyclable catalyst for reduction of 4-nitrophenol, Mater. Chem. Phys. 225 (2019) 42–49.

[24] Z.L. Wu, L. Li, Y.B. Mu, X.B. Wan, Synthesis and adhesive property study of a mussel-inspired adhesive based on poly(vinyl alcohol) backbone, Macromol. Chem. Phys. 218 (16) (2017) 201700206.

[25] X. Jing, H. Li, H.Y. Mi, Y.J. Liu, P.Y. Feng, Y.M. Tan, L.S. Turng, Highly transparent, stretchable, and rapid self-healing polyvinyl alcohol/cellulose nanofibril hydrogel sensors for sensitive pressure sensing and human motion detection, Sens. Actuators B Chem. 295 (2019) 159–167.

[26] Q. Chen, X.N. Yan, H. Lu, N. Zhang, M.M. Ma, Programmable polymer actuators perform continuous helical motions driven by moisture, Acs Appl. Mater. Inter. 11 (2019) 20473–20481.

[27] C. Zheng, C.Y. Liu, H.L. Chen, N. Wang, X. Liu, G.Z. Sun, W.H. Qiao, Effective wound dressing based on poly (vinyl alcohol)/dextran-aldehyde composite hydrogel, Int. J. Biol. Macromol. 132 (2019) 1098–1105.

[28] G. Tao, Y.J. Wang, R. Cai, H.P. Chang, K. Song, H. Zuo, P. Zhao, Q.Y. Xia, H.W. He, Design and performance of sericin/poly(vinyl alcohol) hydrogel as a drug delivery carrier for potential wound dressing application, Mat. Sci. Eng. C-Mater. 101 (2019) 341–351.

[29] O.Y. Kweon, S.K. Samanta, Y. Won, J.H. Yoo, J.H. Oh, Stretchable and self-healable conductive hydrogels for wearable multimodal touch sensors with thermoresponsive behavior, Acs Appl. Mater. Inter. 11 (2019) 26134–26143.

[30] S. Liu, R. Zheng, S. Chen, Y. Wu, H. Liu, P. Wang, Z. Deng, L. Liu, A compliant, self-adhesive and self-healing wearable hydrogel as epidermal strain sensor, J. Mater. Chem. C 6 (15) (2018) 4183–4190.

[31] X. Jing, H. Li, H.Y. Mi, Y.J. Liu, P.Y. Feng, Y.M. Tan, L.S. Turng, Highly transparent, stretchable, and rapid self-healing polyvinyl alcohol/cellulose nanofibril hydrogel sensors for sensitive pressure sensing and human motion detection, Sens. Actuators B Chem. 295 (2019) 159–167.

[32] M. Wang, Y. Chen, R. Khan, H. Liu, C. Chen, T. Chen, R. Zhang, H. Li, A fast self-healing and conductive nanocomposite hydrogel as soft strain sensor, Colloids Surf., A 567 (2019) 139–149.

[33] Y. Li, H. Zhang, S. Ni, H. Xiao, In situ synthesis of conductive nanocrystal cellulose/polypyrrole composite hydrogel based on semi-interpenetrating network, Mater. Lett. 232 (2018) 175–178.

[34] B. Tasdelen, Conducting hydrogels based on semi-interpenetrating networks of polyaniline in poly(acrylamide-co-itaconic acid) matrix: synthesis and characterization, Polym. Adv. Technol. 28 (12) (2017) 1865–1871.

[35] American Society for Testing and Materials (ASTM D638), Standard Test Method for Tensile Properties of Plastics.

[36] Z. Jing, Q. Zhang, Y.Q. Liang, Z. Zhang, P. Hong, Y. Li, Synthesis of poly(acrylic acid)-Fe^{3+}/gelatin/poly(vinyl alcohol) triple-network supramolecular hydrogels with high toughness, high strength and self-healing properties, Polym. Int. 68 (10) (2019) 1710–1721.

[37] B. Lu, H. Yuk, S. Lin, N. Jian, K. Qu, J. Xu, X. Zhao, Pure PEDOT:PSS hydrogels, Nat. Commun. 10 (2019) 1043.

[38] J. James, G.V. Thomas, K.P. Pramoda, N. Kalarikkal, S. Thomas, Thermoplastic-elastomer composition based on an interpenetrating polymeric network of styrene butadiene rubber-poly(methyl methacrylate) as an efficient vibrational damper, New J. Chem. 42 (2018) 1939–1951.

[39] I. Cruz-Cruz, M. Reyes-Reyes, M.A. Aguilar-Frutis, A.G. Rodriguez, R. Lopez-Sandoval, Study of the effect of DMSO concentration on the thickness of the PSS insulating barrier in PEDOT:PSS thin films, Synthetic Met 160 (2010) 1501–1506.

[40] O.P. Dimitriev, D.A. Grinko, Y.V. Noskov, N.A. Ogurtsov, A.A. Pud, PEDOT:PSS films-effect of organic solvent additives and annealing on the film conductivity, Synthetic Met 159 (2009) 2237–2239.

[41] J.I. Daza Agudelo, M.R. Ramirez, E.R. Henquin, I. Rintoul, Modelling of swelling of PVA hydrogels considering non-ideal mixing behaviour of PVA and water, J. Mater. Chem. B 7 (2019) 4049–4054.

[42] S. Luo, X. Qiao, Q.Y. Wang, Y.F. Zhang, P. Fu, Z.D. Lin, F.P. Du, C. Cheng, Excellent self-healing and antifogging coatings based on polyvinyl alcohol/hydrolyzed poly (styrene-co-maleic anhydride), J. Mater. Sci. 54 (2019) 5961–5970.

[43] F.P. Du, N.N. Cao, Y.F. Zhang, PEDOT:PSS/graphene quantum dots films with enhanced thermoelectric properties via strong interfacial interaction and phase separation, Sci. Rep-UK 8 (1) (2018) 6441.

[44] M.D.S. Klem, R.M. Morais, R.J. Goncalves Rubira, N. Alves, Paper-based supercapacitor with screen-printed poly (3, 4-ethylene dioxythiophene)-poly (styrene sulfonate)/multiwall carbon nanotube films actuating both as electrodes and current collectors, Thin Solid Films 669 (2019) 96–102.

[45] H.Y. Du, Z. Song, J.J. Wang, Z.H. Liang, Y.H. Shen, F. You, Microwave-induced shape-memory effect of silicon carbide/poly(vinyl alcohol) composite, Sensor. Actuat. A-Phys. 228 (2015) 1–8.

[46] F. Wang, S.S. Kim, C.D. Kee, Y.D. Shen, I.K. Oh, Novel electroactive PVA-TOCN actuator that is extremely sensitive to low electrical inputs, Smart Mater. Struct. 23 (7) (2014), 074006.

[47] D.A. Gopakumar, V. Arumughan, Y.B. Pottathara, K.S. Sisanth, D. Pasquini, M. Bracic, B. Seantier, A. Nzihou, S. Thomas, S. Rizal, H. Khalil, Robust superhydrophobic cellulose nanofiber aerogel for multifunctional environmental applications, Polym. Basel 11 (2019) 11030495.

[48] M.F. Lin, T.M. Don, F.T. Chang, S.R. Huang, W.Y. Chiu, Preparation and properties of thermoresponsive and conductive composite fibers with core-sheath structure, J. Polym. Sci., Polym. Chem. Ed. 54 (9) (2016) 1299–1307.

[49] M.A. Poothanari, J. Abraham, N. Kalarikkal, S. Thomas, Excellent electromagnetic interference shielding and high electrical conductivity of compatibilized polycarbonate/polypropylene carbon nanotube blend nanocomposites, Ind. Eng. Chem. Res. 57 (2018) 4287–4297.

[50] T. Sharika, J. Abraham, P.M. Arif, S.C. George, N. Kalarikkal, S. Thomas, Excellent electromagnetic shield derived from MWCNT reinforced NR/PP blend nanocomposites with tailored microstructural properties, Compos. B Eng. 173 (15) (2019) 106798.

[51] S. Tanpichai, K. Oksman, Cross-linked nanocomposite hydrogels based on cellulose nanocrystals and PVA: mechanical properties and creep recovery, Compos. Part A-Appl. S. 88 (2016) 226–233.

[52] N. Cai, C. Li, X.G. Luo, Y.N. Xue, L. Shen, F.Q. Yu, A strategy for improving mechanical properties of composite nanofibers through surface functionalization of fillers with hyperbranched polyglycerol, J. Mater. Sci. 51 (2016) 797–808.

[53] X. Fan, W.Y. Nie, S.H. Tsai, N.X. Wang, H.H. Huang, Y.J. Cheng, R.J. Wen, L.J. Ma, F. Yan, Y.G. Xia, PEDOT:PSS for flexible and stretchable electronics: modifications, strategies, and applications, Adv. Sci. 6 (19) (2019) 201900813.

[54] C. Shao, M. Wang, L. Meng, H. Chang, B. Wang, F. Xu, J. Yang, P. Wan, Mussel-inspired cellulose nanocomposite tough hydrogels with synergistic self-healing, adhesive, and strain-sensitive properties, Chem. Mater. 30 (2018) 3110–3121.

[55] T. Wang, Y. Zhang, Q. Liu, W. Cheng, X. Wang, L. Pan, B. Xu, H. Xu, A self-healable, highly stretchable, and solution processable conductive polymer composite for ultrasensitive strain and pressure sensing, Adv. Funct. Mater. 28 (7) (2018) 1705551.

[56] Q.H. Wang, X.F. Pan, C.M. Lin, D.Z. Lin, Y.H. Ni, L.H. Chen, L.L. Huang, S.L. Cao, X. J. Ma, Biocompatible, self-wrinkled, antifreezing and stretchable hydrogel-based wearable sensor with PEDOT:sulfonated lignin as conductive materials, Chem. Eng. J. 370 (2019) 1039–1047.

[57] G. Cai, J. Wang, K. Qian, J. Chen, S. Li, P.S. Lee, Extremely stretchable strain sensors based on conductive self-healing dynamic cross-links hydrogels for human-motion detection, Adv. Sci. 4 (2) (2017) 201600190.

[58] N.S. Liu, G.J. Fang, J.W. Wan, H. Zhou, H. Long, X.Z. Zhao, Electrospun PEDOT: PSS-PVA nanofiber based ultrahigh-strain sensors with controllable electrical conductivity, J. Mater. Chem. 21 (47) (2011) 18962–18966.

[59] Y.J. Liu, W.T. Cao, M.G. Ma, P. Wan, Ultrasensitive wearable soft strain sensors of conductive, self-healing, and elastic hydrogels with synergistic "soft and hard" hybrid networks, Acs Appl. Mater. Inter. 9 (30) (2017) 25559–25570.

[60] M.J. Yee, N.M. Mubarak, M. Khalid, E.C. Abdullah, P. Jagadish, Synthesis of polyvinyl alcohol (PVA) infiltrated MWCNTs buckypaper for strain sensing application, Sci. Rep-UK 8 (2018) 17295.